

Multimodality vascular imaging phantoms: A new material for the fabrication of realistic 3D vessel geometries

Louise Allard

Laboratory of Biorheology and Medical Ultrasonics, University of Montreal Hospital Research Center (CRCHUM), Montréal, Québec H2L 2W5, Canada

Gilles Soulez

Department of Radiology, University of Montreal Hospital (CHUM), Montréal, Québec H2L 4M1, Canada and Department of Radiology, Radio-Oncology and Nuclear Medicine, University of Montreal, Montréal, Québec H3T 1J4, Canada

Boris Chayer, François Treyve, and Zhao Qin

Laboratory of Biorheology and Medical Ultrasonics, University of Montreal Hospital Research Center (CRCHUM), Montréal, Québec H2L 2W5, Canada

Guy Cloutier^{a)}

Laboratory of Biorheology and Medical Ultrasonics, University of Montreal Hospital Research Center (CRCHUM), Montréal, Québec H2L 2W5, Canada; Department of Radiology, Radio-Oncology and Nuclear Medicine, University of Montreal, Montréal, Québec H3T 1J4, Canada; and Institute of Biomedical Engineering, University of Montreal, Montréal, Québec H3T 1J4, Canada

(Received 8 January 2009; revised 7 May 2009; accepted for publication 11 June 2009; published 15 July 2009)

Multimodality vascular flow phantoms provide a way of testing the geometric accuracy of clinical scanners and optimizing acquisition protocols with easy reproducibility of experimental conditions. This article presents a stereolithography method combined with a lost-material casting technique that eliminates metal residues of cerrolow (a low temperature melting point metallic alloy) left within irregular vessel lumens after casting. These residues potentially cause image artifacts especially in magnetic resonance angiography or flow disturbance. Geometrical accuracies of constructed lumens with isomalt, the proposed material, ranged from 3.3% to 5.7% for vessel diameters of 1.8–7.9 mm, which are comparable to those of lumens constructed with cerrolow that had better accuracies varying from 1.1% to 4.1% ($p < 0.02$). Examples of geometries mimicking diseased arteries such as an aorta with stenosed renal arteries and an iliac artery with multiple stenoses are presented. This sugar-based isomalt material, combined with phantom designs having fiducial markers visible in digital subtraction angiography, computed tomography angiography, magnetic resonance angiography, and ultrasound [Med. Phys. **31**, 1424–1433 (2004)], makes easier the fabrication of complex realistic and accurate replicas of pathological vessels with lumen irregularities. © 2009 American Association of Physicists in Medicine. [DOI: [10.1118/1.3171692](https://doi.org/10.1118/1.3171692)]

Key words: vascular flow phantoms, image calibration, ultrasonography, magnetic resonance imaging, x-ray angiography and computerized tomography

I. INTRODUCTION

Developments in manufacturing vascular phantoms have allowed fabrication of geometrical replicas of diseased vessels from 3D medical images. Flow phantoms have been used to study hemodynamics around vascular pathologies, to calibrate radiological 3D imaging technologies, to optimize acquisition parameters and image reconstruction algorithms, and to evaluate imaging artifacts produced by endovascular medical devices to name a few examples. Stereolithography, combined with lost-material casting techniques, has become widely used to produce realistic models of vascular diseases. These technologies offer geometric flexibility and accuracy at an affordable cost.^{1–3} Because of its strength, ease of removal from the mold, and great accuracy ($-0.5%$ in diameter or -0.04 ± 0.06 mm),⁴ the cerrolow metallic alloy with a low melting point temperature is considered an excellent strategy to mold the lumen of simple vessels (the lumen is

produced following the removal of cerrolow).⁵ However, metal residues can be left on the inner surface of the lumen and this problem grows in importance as casting geometries become complex including multiple asperities as observed in atheromatous disease. These residues are problematic, causing imaging or flow artifacts, especially in magnetic resonance imaging (MRI).

The use of wax as the substance in the lost-material casting technique, a method adapted from dentistry prosthetic devices,⁶ can be an interesting alternative to cerrolow. It offers great flexibility to mold complex geometries, its dimensional accuracy is acceptable (between 4% and 10%),^{3,7,8} and potential residues of wax have little impact on imaging techniques but may affect flow. However, wax reproductions are very fragile and small diameter vessels (e.g., less than 2 mm) cannot be designed.⁸ The surface finish is poorer than that of cerrolow; additional finishing and polishing might be neces-

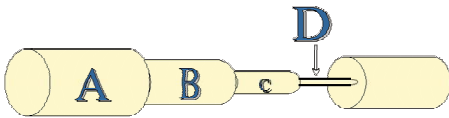


FIG. 1. Rod molded 20 times with cerrolow and isomalt. The diameter of four different segments (A, B, C, and D) was measured five times for each rod with a microcaliper. Rotation of the rod assured independent measures. The diameters of the four segments of the brass positive were, respectively, 7.90, 5.03, 3.18, and 1.84 mm.

sary before applying a polymer to often mimic the vessel wall. Because the wax has to be removed thermally and chemically, this process may deteriorate certain wall mimicking polymers and deform the vessel geometry.

It appears from the above review that there is still a need for the development of a new fabrication process that allows enough flexibility to build realistic vessels, presents a good geometric accuracy, and supports small diameter vessels, without metal residues. Isomalt, a commercial sugar alcohol widely used as a sweetener, is a promising alternative. This white crystalline substance also found applications in pharmaceutical preparations of tablets, capsules, coatings, candies, and many more. The commercially available isomalt in granules can be thermally melted to obtain a liquid for molding, has a low hygroscopicity, and can easily produce small or large pieces.⁹ At room temperature once crystallized, this material has a glassy state allowing the production of a rigid skeleton for phantom design. For the application considered here, the crystallized molded isomalt is dissolved in water at room temperature to create the empty vessel lumen mimicking a human artery. The purpose of this study was to test isomalt as a new material to create complex geometries of vascular pathologies and to compare the accuracy of the fabrication process to that obtained with cerrolow.

II. MATERIAL AND METHODS

II.A. Geometric accuracy of the vessel lumen diameter

The geometric accuracy following molding of isomalt and cerrolow was tested by comparing diameters of a micromachined brass positive rod (a brass rod with four different diameters—see Fig. 1) that was used to create the master silicone mold to diameters of 20 isomalt and 20 cerrolow rods cast in the mold. To prepare isomalt rods, the sugar-based granules (Farinex, Boisbriand, QC, Canada) were melted at a temperature between 145 and 150 °C and poured into the two-part silicone mold. After casting, the isomalt core was cooled at room temperature for 20 min (the solidification temperature of isomalt is 60 °C, according to Ref. 10) then extracted from the mold and slightly hand polished to remove surface irregularities at the mold junction. The cerrolow bars were prepared with a 58 °C melting point cerroindium alloy core (cerrolow 136, Cerrometal Products, Bellefonte, PA) and cast in the same mold with sections at different diameters. Then, the metallic core was cooled at room temperature for 2 h before being removed and slightly hand polished at the mold junction. At four different posi-

tions along the isomalt and cerrolow rods (see Fig. 1), the diameter was measured five times by using a microcaliper following rotation of the rod.

II.B. Molding complex and irregular geometries with isomalt and cerrolow

Molded realistic geometries were replicas of human multidetector computed tomography (MDCT) scans of patients with obstructed renal arteries and an iliac artery with multiple stenoses. To recover the 3D geometry, the luminal boundary of each cross section was semiautomatically segmented with SLICEOMATIC (version 4.2, TomoVision Inc., Montreal, QC, Canada) by considering the image gradient. The reconstructed 3D vessel was validated by an expert radiologist and a VRML (virtual reality modeling) file was exported for each geometry to further be processed with the IMEdit module of POLYWORKS (version 8.1, InnovMetric Inc., Quebec, QC, Canada). This last software was used to smooth and resample contours and to produce a STL output file compatible with stereolithography. An epoxy resin skeleton representing the smoothed surface of each vascular pathology was generated by stereolithography (Dorval Technologies, Montreal, QC, Canada) with a resolution of 125 μm . This positive geometry was then used to create the master silicone mold (i.e., negative mold) in which the vascular skeletons made of isomalt or cerrolow were cast. Vascular phantoms were then prepared according to the manufacturing process described previously.⁴ A slight modification to this protocol was made; a thin polyurethane membrane (Product No. ren-6400-1, Huntsman International, Mississauga, ON, Canada) was painted on the vessel skeleton instead of latex. This polyurethane is invisible in MRI and CT, produces acceptable specular reflection and attenuation in ultrasound, and it was selected to increase the long-term durability of our phantoms (latex degraded over time). Fiducial markers visible in digital subtraction angiography (DSA), CT, MRI, and ultrasound were embedded in the mimicking tissue material (agar gel with antibacterial) surrounding the vessel and filling the phantom's box. The characteristics of these markers and the method used to precisely position them around the vessel lumen were described previously.⁴

To create the vessel lumen, the vertically oriented phantom was immersed in a water bath at room temperature for 2–3 h. The isomalt dissolved and was then removed from the phantom via its inlet and outlet tube connectors to create in the agar gel a conduit with a polyurethane wall having the shape of the initial core.

II.C. Image acquisitions for validation

A further validation step consisted of comparing lumen irregularities of the renal artery phantoms in an attempt to demonstrate the absence of molding residues with isomalt, which could cause image artifacts. For this purpose, two vascular flow phantoms were constructed using isomalt and cerrolow as the casting material.

DSA image acquisitions of these vascular phantoms were performed by using standard clinical protocols. Digital spot

TABLE I. Average diameters of the isomalt and cerrolow rods at four different sections identified in Fig. 1. The number of rods was 20 per group.

Positions on the rod	Brass positive (mm)	Cerrolow percentage error (difference in mm)	Isomalt percentage error (difference in mm)
A	7.90	-1.8% (-0.14 ± 0.07)	-3.7% (-0.29 ± 0.08) ^{a,b}
B	5.03	-3.2% (-0.16 ± 0.05) ^a	-5.4% (-0.27 ± 0.06) ^{a,b}
C	3.18	-4.1% (-0.13 ± 0.05)	-5.7% (-0.18 ± 0.04) ^{a,b}
D	1.84	-1.1% (-0.02 ± 0.03)	-3.3% (-0.06 ± 0.04) ^{a,c}

^a $p < 0.05$, comparison with analysis of variance tests of the average error diameter of the rod made with cerrolow or isomalt with the brass positive rod dimension.

^b $p < 0.001$, comparison with Mann-Whitney rank sum tests of the average diameter of the rod made with cerrolow and isomalt.

^c $p = 0.02$, comparison with a Mann-Whitney rank sum test of the average diameter of the rod made with cerrolow and isomalt.

film acquisitions at 0° and 45° right-anterior-oblique (RAO) and left-anterior-oblique (LAO) projections of the phantom made with cerrolow were performed on an Angiorex CAS-10-DFP-2000 unit (Toshiba, Tokyo, Japan) by using the following parameters: field of view=17 cm, tube-intensifier distance=100 cm, table height=80 cm, matrix size=1024 × 1024, current intensity=400 mA, and peak voltage =70 kV, while one shot projections of the phantom made with isomalt were done on an Axiom Artis DTA unit (Siemens, Forchheim, Germany) by using the same acquisition parameters. Different angiography units were used for the phantom acquisitions because the Angiorex system had been replaced. The vessels of both vascular phantoms were filled with air instead of contrast solution to keep the vascular lumen clear to better appreciate potential residues left.

To demonstrate the multimodality imaging capability of isomalt (i.e., absence of imaging artifacts in DSA, CT, MRI, and B-mode ultrasound), another vascular flow phantom mimicking an iliac artery with multiple stenoses was constructed. All image acquisitions of this last phantom were also performed by using standard clinical protocols. DSA acquisitions were obtained with the Axiom Artis unit by using the same parameters chosen to image the renal artery phantom. This phantom was filled with a contrast solution of iohalamate meglumine at 141 mg/ml (Conray 30, Mallinckrodt Medical, Pointe-Claire, QC, Canada). For CT, the phantom was imaged with a Somatom Sensation 64-slice scanner (Siemens, Erlangen, Germany) by using a slice thickness of 1 mm, a pitch of 0.7 mm, and a reconstruction interval of 0.7 mm. The vessel lumen was filled with a 2.8% v/v (volume concentration) solution of 430 mg/ml iohalamate meglumine (Conray 43, Mallinckrodt Medical, Pointe-Claire, QC, Canada) diluted in a 0.9% NaCl solution. Other parameters for CT angiography (CTA) scans were a current of 217 mA, a peak voltage of 120 kV, a matrix size of 512 × 512, and a field of view of 38 cm. MR angiography (MRA) imaging was performed with a 1.5 T unit (Avento, Siemens, Erlangen, Germany). The phantom vessel was filled with 3.6 ml of 0.5 mole/l gadopentetate dimeglumine solution (Prohance, Bracco Diagnostics, Princeton, NJ) diluted in 100 ml of 0.9% NaCl solution giving a 1.8 mmole/l concentration. A high resolution three-dimensional fast low angle shot

(FLASH) sequence in the coronal plane using a body array coil was used (repetition time=3.2 ms, echo time=1.1 ms, flip angle=30°, field of view=281 × 375 mm², matrix size =384 × 512). Finally, a Vivid Five ultrasound scanner (General Electric Medical Systems, Milwaukee, WI) with a 50 × 17 mm² 192 elements linear array probe (FLA 10 MHz) was used to collect B-mode cross-sectional images at 10 MHz. The vessel lumen was filled with degassed water to allow ultrasound transmission. All multimodality imaging acquisitions were performed at room temperature and a lumen pressure of 20 mm Hg was applied to allow filling of the contrast agent or degassed water in all vessel sections of the phantoms. A syringe coupled with a manometer allowed maintaining this static pressure. No flow was circulated in any phantom during image acquisitions.

III. RESULTS

III.A. Geometric accuracy of the vessel lumen diameter

As shown in Table I, the dimension agreement of cerrolow rods to that of the brass positive (maximum relative mean error of -4.1%) was better than that of isomalt (-5.7%). For cerrolow, analysis of variance tests revealed a significant difference between the positive dimension and cerrolow bars for segment B only ($p < 0.05$), whereas for isomalt, differences were significant for all segments ($p < 0.05$). Mann-Whitney rank sum tests to compare cerrolow and isomalt moldings showed significant differences in diameter measurements for all positions along the rods ($p < 0.001$ for positions A, B, and C and $p = 0.02$ for D). A general tendency observed for both materials was that the amount of shrinking that occurred during molding was directly proportional to the size of the vessel.

III.B. Molding complex and irregular geometries with isomalt and cerrolow

Figure 2 illustrates the efficacy of isomalt to fabricate complex realistic replicas of pathological vessels with lumen irregularities. The visual assessment of panels (C) and (D) obtained with DSA reveals that the phantom prepared with

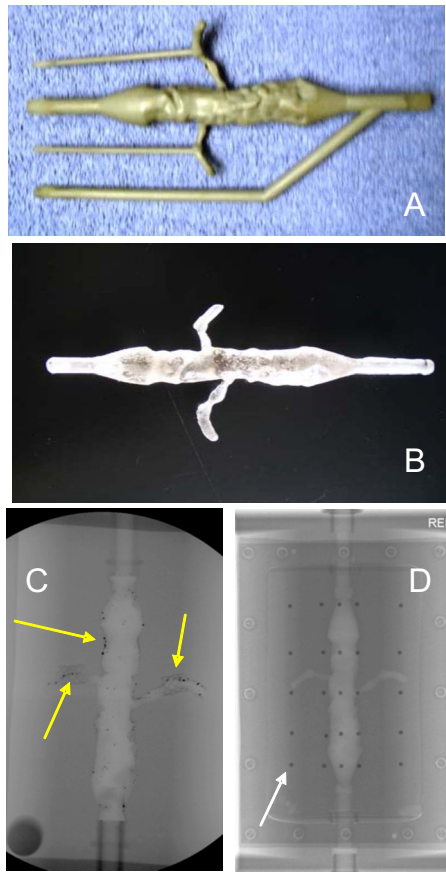


FIG. 2. (A) Resin skeleton mimicking a human aorta with obstructed renal arteries obtained by stereolithography. (B) Isomalt core. DSA of vascular flow phantoms molded with the (C) cerrow alloy and (D) isomalt. Arrows in (C) indicate cerrow residues. The arrow in (D) shows 1 of 25 fiducial markers embedded in the phantom. Note that the phantom in (C) was made without spherical markers.

cerrow [panel (C)] had metal residues left on the vessel wall after melting (yellow arrows), whereas the vessel wall of the phantom prepared with isomalt was free of any x-ray metallic absorption. These residues of cerrow were left on the polyurethane vessel wall even though the lumen had been washed thoroughly with hot water at a temperature well above the melting point of 58 °C. Note in Fig. 2 that the phantom made with cerrow [panel (C)] did not include fiducial markers visible as spherical black dots on panel (D).

Figure 3 provides other opportunities to judge the quality of complex vascular moldings with distributed atherosclerotic stenoses obtained with isomalt. The DSA image in panel (B) clearly shows diffused stenoses on the iliac artery, the 2D projection of 25 fiducial markers, and the inlet and outlet of the flow phantom. Note that one branch of the aortoiliac bifurcation was left intentionally cut. The 2D projections in panels (C) and (D) allow to identify 5 of the 25 fiducial markers as hyperdense dots in CTA and hypointense dots in MRA. An ultrasound image plane showing the tightest stenosis is presented in panel (E). Note that the polyurethane vessel wall is identifiable from the tissue-mimicking background. One fiducial marker is also visible at the bottom of the image at the level of the most severe stenosis. No

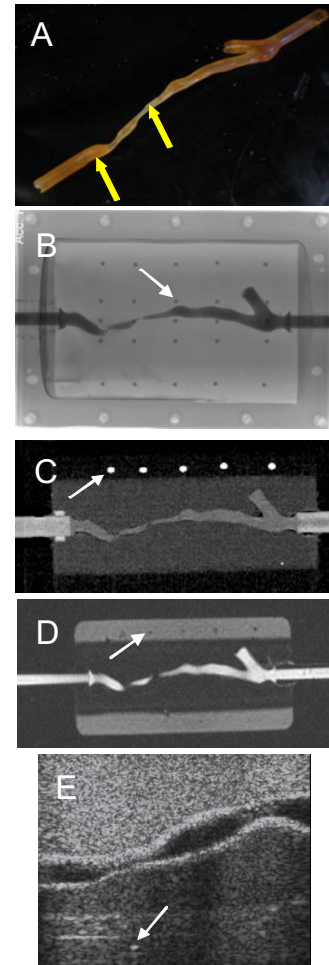


FIG. 3. (A) Resin skeleton mimicking a human iliac artery with diffused stenoses obtained by stereolithography. Images of the vascular phantom molded with isomalt and scanned in (B) DSA, (C) CTA, (D) MRA, and (E) B-mode ultrasound. Positions of some fiducial markers in (B) to (E) are indicated by arrows. Arrows in panel (A) indicate the subregion of panel (E).

undesirable image distortion or artifacts have been noted in either DSA, CTA, MRA, or B-mode ultrasound, as reported previously.⁴

IV. DISCUSSION

According to Table I, it can be concluded that the geometric accuracy of cylindrical vessels made with cerrow is excellent with errors typically below 4% but that of isomalt remains acceptable when compared with wax. Indeed, the percentages of error obtained with isomalt ranged from 3.3% to 5.7%, which are smaller than values reported in the literature for the lost-wax material with errors varying between 4% and 10%.⁷ Up to now, wax was the only lost-material alternative to cerrow.

The differences in geometric accuracies reported in Table I for isomalt and cerrow can be interpreted by considering the volumetric coefficient of thermal expansion (CTE) of the silicone mold, which should be close to $15 \times 10^{-6} / ^\circ\text{C}$.¹¹ Qualitatively, because cerrow has a melting point of 58 °C, while that of isomalt is 147 °C, the larger dissipation of heat required to cool isomalt rods likely resulted in larger

volume expansions of the mold. Consequently, when liquid isomalt was poured, the actual inner lumen diameter dimensions of the mold decreased and larger negative errors occurred compared with cerrolow (larger underestimations of the “gold standard” brass rod dimensions).

Another interesting observation can be made in relation with the CTE of the mold. In the current study, the error difference for molding a 7.9 mm diameter cerrolow rod was -1.8% (see Table I), whereas it was only -0.5% in a previous study⁴ ($p=0.016$ based on a paired t-test that included all measurements of both studies). Note that we cannot compare other diameters reported in Table I because only a 7.9 mm segment of an axisymmetric double stenosis model was tested in that previous study of our group. In Ref. 4 cerrolow rods were fabricated in an aluminum mold with a CTE of approximately $23.1 \times 10^{-6}/^{\circ}\text{C}$,¹² which is slightly higher than that of silicone. Consequently, the smaller errors reported previously in Ref. 4 cannot be attributed to this physical effect because a larger expansion of the mold would have been expected with aluminum when compared with silicone. The larger errors of the current study must thus be attributed to differences in precision of the mold. In Ref. 4 the aluminum mold was micromachined whereas the silicone mold was fabricated in-house by using the brass rod as the footprint. Although larger errors were observed in the current study, note that silicone is flexible which makes easier demolding of complex geometries compared with aluminum mold.

Intriguingly at a first glance, it can be observed in Table I for both isomalt and cerrolow that except for one measure, the difference (in mm) between the mean diameter of the molded cores and that of the brass positives was more important as the dimension of the segment (A to D) is enlarged; the difference (in mm) was larger due to shrinkage for the larger diameter segments. Cerrolow produces very low shrinkage casting cores,⁴ whereas the volume stability of isomalt seemed in our study to be influenced by the rapidity of cooling and heating. As mentioned by Borde and Cesàro,^{10,13} to reduce volume shrinkage during cooling (to produce the rigid core), the temperature dissipation gradient should be the same as the one used to heat the isomalt granules to liquefy them (to cast isomalt into the mold). The rate of cooling and heating could not be easily controlled in this study. Indeed, considering the rod diameters in Fig. 1, the rate of cooling was likely different depending on the diameter of the rod and thus the quantity of isomalt in the mold. This factor may thus have contributed to error differences in Table I. This issue can also be extended to compare molding in silicone versus aluminum. According to Huan and Jordaan,¹⁴ products casted in silicone molds experience undesired shrinkage and porosity because even if silicone rubber molds can withstand a temperature of 420°C , this material has a low thermal conductivity of typically $0.23 \text{ W/m}^{\circ}\text{C}$.¹¹ Because the conductivity of aluminum is quite high [$237 \text{ W/m}^{\circ}\text{C}$ (Ref. 12)], the rate of cooling is much faster and this would likely reduce shrinking of isomalt (similar dissipation temperature gradient between heating of granules and cooling of molded geometries). However, be-

cause aluminum is not flexible and isomalt is fragile, this is not an avenue that should be privileged to facilitate demolding.

Combined with the manufacturing process proposed previously by us⁴ to produce multimodality vascular imaging phantoms with fiducial markers, the isomalt lost-material casting technique offers the possibility to accurately mold complex geometries at an affordable cost. Moreover, because isomalt is a crystalline substance that totally dissolves in water at room temperature, removal of this lost-casting material creates in the gel a conduit with a polyurethane wall containing no residues potentially causing imaging or flow artifact.

Up to now, this phantom design has been used for many applications, namely, as a tool for the calibration and fusion of multimodality images of cylindrical vessels,¹⁵ to optimize peripheral MRA acquisition parameters for the purpose of quantifying peripheral vascular stenoses,¹⁶ to evaluate the performance of a new prototype medical ultrasound scanning robot for lower limb vascular applications,¹⁷ to quantify in-stent restenoses with 3D B-mode and power Doppler ultrasound imaging,¹⁸ and to optimize MRI acquisition protocols using intravascular antenna.¹⁹ Finally, a nitinol stent with tantalum markers was implanted in the structure of the vascular phantom to evaluate artifacts produced on MRA and CTA imagings.²⁰

V. CONCLUSIONS

A new lost material for manufacturing multimodality vascular imaging phantoms was presented. Isomalt is an interesting alternative to cerrolow in creating accurate vascular phantoms of realistic complex pathologies. This new lost material can be used favorably with geometries having lumen asperities, because no residues creating image artifacts are left on the vessel wall during molding.

ACKNOWLEDGMENTS

This work was supported by grants from the Canadian Institutes of Health Research (Grant No. MOP-53244) and the Vinci Program of the University of Montreal that was financially supported by Valorisation-Recherche Québec. Dr. Soulez and Dr. Cloutier are, respectively, recipients of a Clinical Scholarship and National Scientist awards of the Fond de la Recherche en Santé du Québec. Thanks to Professor Yves Petit of the Institut de tourisme et d'hôtellerie du Québec for helpful discussions on isomalt properties.

^{a)} Author to whom correspondence should be addressed. Electronic mail: guy.cloutier@umontreal.ca

¹R. V. Yedavalli, F. Loth, A. Yardimci, W. F. Pritchard, J. N. Oshinski, L. Sadler, F. Charbel, and N. Alperin, “Construction of a physical model of the human carotid artery based upon in vivo magnetic resonance images,” *J. Biomed. Eng.* **123**, 372–376 (2001).

²E. Berry, A. Marsden, K. W. Dalgarno, D. Kessel, and D. J. A. Scott, “Flexible tubular replicas of abdominal aortic aneurysms,” *Proc. Inst. Mech. Eng., Part H: J. Eng. Med.* **216**, 211–214 (2002).

³K. Knox, C. W. Kerber, S. A. Singer, M. J. Bailey, and S. G. Imbesi, “Stereo lithographic vascular replicas from CT scan: Choosing treatment strategies, teaching, and research from live patient scan data,” *AJNR Am. J. Neuroradiol.* **26**, 1428–1431 (2005).

- ⁴G. Cloutier, G. Soulez, S. Qanadli, P. Teppaz, L. Allard, Z. Qin, F. Cloutier, and L. G. Durand, "A multimodality vascular imaging phantom with fiducial markers visible in DSA, CTA, MRA, and ultrasound," *Med. Phys.* **31**, 1424–1433 (2004).
- ⁵R. F. Smith, B. K. Rutt, and D. W. Holdsworth, "Anthropomorphic carotid bifurcation phantom for MRA applications," *J. Magn. Reson. Imaging* **10**, 533–544 (1999).
- ⁶M. Horacek, "Accuracy of castings manufactured by the lost wax process," *Foundry Trade J.* **171**, 423–424 (1997).
- ⁷P. Gailloud, M. Muster, M. Piotin, F. Mottu, K. J. Murphy, J. H. D. Fasel, and D. A. Rufenacht, "In vitro models of intracranial arteriovenous fistula for the evaluation of new endovascular treatment materials," *AJNR Am. J. Neuroradiol.* **20**, 291–295 (1999).
- ⁸S. G. Wetzel, M. Ohta, A. Handa, J. M. Auer, P. Lylyk, K. O. Lovblad, D. Babic, and D. A. Rufenacht, "From patient to model: Stereolithographic modeling of the cerebral vasculature based on rotational angiography," *AJNR Am. J. Neuroradiol.* **26**, 1425–1427 (2005).
- ⁹J. Raudonus, J. Bernard, H. Janben, J. Kowalczyk, and R. Carle, "Effect of oligomeric or polymeric additives on glass transition, viscosity and crystallization of amorphous isomalt," *Food Res. Int.* **33**, 41–51 (2000).
- ¹⁰B. Borde and A. Cesàro, "A DSC study of hydrated sugar alcohols," *J. Therm. Anal. Calorim.* **66**, 179–195 (2001).
- ¹¹<http://www.efunda.com>. Consulted in May 2009.
- ¹²<http://hypertextbook.com/physics/thermal>. Consulted in May 2009.
- ¹³B. Borde and A. Cesàro, "Thermal properties of isomalt: A diastereomer mixture," *J. Therm. Anal. Calorim.* **69**, 267–280 (2002).
- ¹⁴Z. Huan and G. D. Jordaan, "Investigation of the cooling of spin-casting moulds," *Appl. Therm. Eng.* **23**, 17–27 (2003).
- ¹⁵N. Boussion, G. Soulez, J. de Guise, M. Daronat, Z. Qin, and G. Cloutier, "Geometrical accuracy and fusion of multimodal vascular images: A phantom study," *Med. Phys.* **31**, 1434–1443 (2004).
- ¹⁶A. Tang, G. Cloutier, E. Therasse, G. Beaudoin, S. Qanadli, M. F. Giroux, N. Boussion, J. de Guise, V. L. Oliva, and G. Soulez, "Optimization of spatial resolution for peripheral magnetic resonance angiography," *Acad. Radiol.* **14**, 54–61 (2007).
- ¹⁷M. A. Janvier, L. G. Durand, M. H. Roy Cardinal, I. Renaud, B. Chayer, P. Bigras, J. de Guise, G. Soulez, and G. Cloutier, "Performance evaluation of a medical robotic 3D-ultrasound imaging system," *Med. Image Anal.* **12**, 275–290 (2008).
- ¹⁸M. Lécart, M. H. Roy Cardinal, Z. Qin, G. Soulez, and G. Cloutier, "In vitro in-stent restenoses evaluated by 3D ultrasound," *Med. Phys.* **36**, 513–522 (2009).
- ¹⁹G. Guilbert, G. Soulez, and G. Beaudoin, "Comparative evaluation of the geometrical accuracy of intravascular magnetic resonance imaging: A phantom study" *Acad. Radiol.* (in press).
- ²⁰L. Létourneau-Guillon, G. Soulez, G. Beaudoin, V. L. Oliva, M. F. Giroux, Z. Qin, N. Boussion, E. Thérasse, J. de Guise, and G. Cloutier, "CT and MR imaging of nitinol stents with radioopaque distal markers," *J. Vasc. Interv. Radiol.* **15**, 615–624 (2004).